Smart materials behavior in phosphates: Role of hydroxyl groups and relevance to antiwear films

Dmitry Shakhvorostov,[1,a)] Martin H. Müser,[1] Yang Song,[2] and Peter R. Norton[2]
[1]*Department of Applied Mathematics, University of Western Ontario, London, Ontario N6A 5B7, Canada*
[2]*Department of Chemistry, University of Western Ontario, London, Ontario N6A 5B7, Canada*

(Received 25 March 2009; accepted 26 June 2009; published online 24 July 2009)

The elastic properties of materials under high pressure are relevant to the understanding and performance of many systems of current interest, for example, in geology and tribology. Of particular interest is the origin of the dramatic increase in modulus with increasing pressure, a response which is also called "smart materials behavior." In this context, simple phosphate-containing materials have been studied experimentally and theoretically, and the origins of this behavior have been associated with factors such as coordination of the cations and changes in the degree of polymerization and hydrogenation of the phosphate units. In the present paper we extend the former analysis on simple metal phosphate model compounds to so-called thermal films, an intermediate stage in the formation of effective antiwear films. The material was produced by heating a commercial zinc dialkyldithiophosphate (ZDDP), a common antiwear additive in lubricating oils, in poly-α-olefin base oil solutions to 150 °C, a process known to produce the thermal films. Its structure and equation of state were studied by means of x-ray diffraction and IR synchrotron radiation techniques during compression up to 25 GPa in a diamond anvil cell as well as during the subsequent decompression. As is the case for the simple metal phosphates, we find that the thermal films are relatively soft at low pressures but stiffen rapidly and ultimately amorphize irreversibly at high pressure. However, in addition to phase transformations involving cation sites occurring in the metal phosphates studied previously, thermal films undergo displacive transitions associated with instabilities of the hydroxyl groups. These results may imply that ZDDP ligands and those of the transformed materials not only affect ZDDP decomposition rate in engines but also the mechanical properties of the resulting antiwear films. © *2009 American Institute of Physics*.
[DOI: 10.1063/1.3182854]

I. INTRODUCTION

Zinc dialkyldithiophosphates (ZDDPs) are widely used additives in commercial lubricants. Their decomposition products form films on metal surfaces, thereby protecting them from wear. They were first introduced as antioxidants. Despite the fact that ZDDPs have been successfully used since the 1940s, their antiwear mechanisms remain a matter of debate.[1–4] Understanding of the function of ZDDPs at a molecular level would help to develop a second generation of antiwear agents, as usage of ZDDPs has to be significantly reduced in the future, due to poisoning of the catalytic converters by sulfur, phosphorus, and zinc. Much of the earlier research on the antiwear film formation has focused on investigation of the chemical pathways of their formation.[3,4] Several mechanisms have been suggested previously that slightly differ in details but follow one general scheme involving three steps in which chemical changes occur: (i) when in solution, (ii) when on the surface, and (iii) when on the surface during rubbing. These are as follows.

(1) Initial ZDDP isomer with an attached ligand (for solubility) is converted to a linkage isomer in the oil solution[5] and/or is adsorbed on the metal surface.[3]
(2) (a) ZDDP reacts with the metallic surface to form species of phosphates and phosphothionic moieties bound to the metal surface[3] or (b) ZDDP or/and linkage isomer decompose(s) by thermal-oxidative processes with oxygen or organic peroxides producing zinc metaphosphate (a long-chain polyphosphate), $Zn(PO_3)_2$, and small amounts of zinc sulphide.[5,6]
(3) (a) With continued rubbing, in the presence of water from the base oil, hydrolysis of polyphosphates occurs, creating short-chain polyphosphates.[3] (b) Depending on the availability of cations (such as Fe) or the magnitude of the reaction temperature, friction induces the formation of either pyrophosphates ($FeZnP_2O_7$) or orthophosphates $Fe_2Zn(PO_4)_2$.[5,6] (c) Eventually friction induces an acid-base reaction between phosphates and iron oxides on the metal surface since Fe^{3+} is a harder Lewis acid than Zn^{2+} and therefore a cation exchange is highly favorable.[7] It is also suggested that the chain length of the polyphosphate structure will decrease with rubbing as Zn^{2+} cations are replaced by the more highly charged Fe^{3+} cations.

The formation of ZDDP-based antiwear films and their action according to the mechanisms given above, depends, among other parameters, on the kinetics of layer formation,

a)Electronic mail: dshakhvo@uwo.ca.

e.g., on the decomposition temperature of ZDDP and its concentration in oil and the type of isomer (neutral, isobutyl, etc.).[8–11] The essence of the results of previous experimental investigations of the antiwear efficiency of ZDDP can be summarized thus: less thermally stable ZDDP isomers which decompose more efficiently and/or the occurrence of higher temperatures in the contact zone will result in more rapid film formation and therefore better antiwear action.

With the development of nanoindentation techniques, much emphasis has also been placed on the response of the antiwear films to stresses, in particular, the correlation of the mechanical properties (modulus and hardness) with film chemistry and structure. Experimental evidence has been provided for dramatic stiffening of the films at elevated pressures (many gigapascals), which is believed to underlie some of their antiwear properties; this is often called "smart materials behavior." (Smart materials behavior is realized when the material responds to an external stimulus in an unusually strong fashion, e.g., its bulk modulus K increases with pressure p not simply in direct proportion to p but by a large multiple of p, i.e., if $dK/dp \gg 1$.) In addition, computational methods have provided completely new insights into how mechanical properties depend on chemical details such as cation coordination and degree of polymerization and hydrogenation.[2,12] Nanoindentation experiments reported in Ref. 13 for films deposited on a steel substrate have indicated that the elastic modulus of the film increases in the process of indentation. Taken at face value, these results show a fundamental possibility of extraordinary stiffening of the film. However, the modeling used an oversimplified two spring model of the film/substrate system for analysis of the experimental data, and this left some room for an alternative explanation of the apparent stiffness increase, i.e., the increasing influence of the stiff substrate during indentation.

Spatially resolved nanoindentation experiments indicated that the antiwear films are stiffer on the tops of the antiwear pads and softer in the valleys.[14,15] The antiwear pads are assumed to form preferentially at the locations of the original asperities at the sliding interfaces, where the contact pressures and flash temperatures will be highest. These findings were correlated with the observation of long-chain polyphosphate structure on the tops of the pads and short-chain structure in the valleys. It was argued that higher stress and/or temperature on the tops of the pads were responsible for the occurrence of longer chain polyphosphates. It was tempting to explain the increased stiffness at these locations by the presence of structures with an increased phosphate chain length. This link, however, was not firmly established, as the increased linear chain length does not necessarily produce an increased stiffness of the material. In addition, depth-resolved spectroscopy of the film indicated a short chain structure near the interface metal/film and long-chain structure at the surface.[6,16,17] Such double layer or gradient structure of the film was also found in thermally produced films formed at a constant reaction temperature, as was shown by infrared (IR) spectroscopy which was used to monitor phosphate chain length during film growth.[18] This study indicated that the double layer structure of the film might be just a function of the reaction time/film thickness and occurs due to either the decrease in the concentration of unreacted ZDDP or to the surface specific polymerization/crystallization kinetics. Support for the latter argument is found in the fact that the short-long chain depth resolved structure of the film can be repeatedly produced, eventually creating four-layered, six-layered, (and so on) structures by exchange of an oil lubricant depleted of ZDDP with a freshly blended ZDDP-oil solution.[19]

The possibility of film stiffening on the tops of the pads was modeled in a set of *ab initio* simulations involving compression of pure phosphates and zinc phosphates with different Zn/phosphate ratios.[2,20,21] Results of the computations indicated that ZDDP films would form more rapidly in the tribological contacts in comparison with films formed under purely thermal activation because of pressure-induced rapid polymerization of the films. It was argued that the stiffening of the zinc phosphates observed on the tops of the pads could be explained by an irreversible pressure-induced cross linking of the phosphate units/chains involving an eventual irreversible increase in the coordination of the zinc cation. It was also argued that the reversible coordination change at the cation site could explain the extraordinary stiffening (smart behavior) observed in the earlier nanoindentation experiments.[13]

Subsequent high pressure experiments[12,22] provided evidence for a reversible pressure-induced cation coordination increase. They also indicated that strong stiffening occurs even *without* coordination change at the cation site. To be specific, nominal values of dK/dp for regular metals and semiconductors are near five,[23–27] but are found to be in the range of 30 in simple metal phosphates.[12] Particularly strong stiffening appears in metal phosphates with low cation coordination or/and presence of groups not participating in the network formation. It was argued that the underlying molecular mechanism of extensive pressure-induced stiffening of phosphates is due to suppression of rigid unit modes[28,29] induced by the displacement of the phosphate groups.

Despite the fact that the mechanism of the stiffening was related to the decrease in the flexibility of rigid unit modes upon compression—with or without change in cation coordination, it remained to be answered if these explanations can be applied to the material making up the antiwear films. Recent experimental and theoretical studies determined the properties of compounds that were chosen as models for the decomposition products of ZDDP, but there is no certainty that these molecules really represent actual compounds present in the transformation of ZDDPs to antiwear film material. For this reason, in the present paper, we present work on thermal films that were formed by heating ZDDP containing poly-α-olefin base oil solutions to 150°. The chemistry and structure of these films closely correspond to the chemistry of the tribofilms produced in low pressure/shear contacts.

We used diamond anvil cell (DAC) high pressure experiments for determination of the bulk modulus of the antiwear films as an alternative to the previously conducted nanoindentation experiments.[13–15] The data should be highly complementary but offer a significant advantage over nanoindentation determination of the modulus. The nanoin-

dentation techniques have been proven to be very accurate when determining the properties of a single-phase bulk material, but investigation of the elastic properties of a thin layer always leaves some uncertainty due to the complexity of the indenter/layer/substrate system. This complexity leads to concomitant difficulties/uncertainties connected with the mathematical treatment of the results to filter out the elastic properties of the thin layer from those of the substrate. In contrast to nanoindentation, the determination of the bulk modulus in high pressure anvil cell experiments is done via direct measurement of the pressure-induced decrease in the unit cell volume in the investigated crystalline structure and can be regarded as one of the most precise techniques to determine the bulk modulus of a specific structure. In addition, x-ray diffraction (XRD) and IR spectroscopy applied *in situ* (during compression) allow one to investigate the molecular details responsible for the specific elastic behavior.

The remainder of this article will be organized as follows. In Sec. II, we describe how we obtain the thermal decomposition products of ZDDP (thermal films) in a form of powder and the use of the diamond-anvil cell to compress them. Section III contains the results from high pressure XRD and IR spectroscopy experiments using synchrotron radiation. Conclusions are drawn in Sec. IV.

II. METHODS

In this study, samples were exposed to isotropic stresses. During compression, the chemical and crystalline structures were analyzed by means of XRD and IR spectroscopy using synchrotron radiation.

A. High pressure equipment and sample preparation

For sample compression, a symmetric piston-cylinder-type of DAC equipped with 400 μm culet diamond anvils was used. A few ruby (Cr^{+3} doped α-Al_2O_3) chips as pressure calibrant were carefully placed inside the gasket sample chamber before the sample was loaded. The pressure was determined from the well known pressure shift in the R_1 ruby fluorescence line (at 694.2 nm under ambient conditions) with an accuracy of ± 0.05 GPa under quasihydrostatic conditions.[30] A custom made Raman spectrometer was used for pressure determination. The spectrometer was calibrated at several absorption lines using diamond and silicon standards to ensure linearity of the wave number scale. Purity of all model phosphates obtained from Aldrich is 99.999% except for $ZnH_2P_2O_7$ hydrate, which was prepared as described in Ref. 31. The structure of the latter was verified using XRD.

A poly-α-olefin base oil and the commercial primary and secondary mixed ZDDP (ECA 6654, 15% *n*-octyl and 85% isobutyl, ESSO Petroleum, Canada) were mixed to obtain 1.2 wt % ZDDP solutions. The resulting solutions where heated at constant temperature of 150 °C for 24 h in the presence of fine iron powder with average particle diameter of 1 μm. The ZDDP decomposition products created a thin layer around the particles resulting in an increase in the average lateral dimensions of ~ 5 μm. Based on relative volumes, the central iron "core" of the average particle should constitute less than 1% of the volume of the entire particle and hence make a negligible contribution to the mechanical or spectroscopic behavior of the system in the DAC experiments. Particles were then washed three times and filtered using hexane solvent. The samples were loaded at room temperature and a relative humidity of 60%–80% as powder with nominal pressure slightly above ambient using silicone oil as a pressure transmitting medium for the XRD experiments and KBr for the IR spectroscopy.

In the course of the compression/decompression procedure, the DAC was carefully pressurized in small steps and allowed to stabilize for a few minutes after each pressure change before XRD data or IR spectra were taken. Maximum pressure in experiments was set to ≈ 25 GPa at room temperature and reproduced a few times.

B. Infrared spectroscopy

IR experiments were performed at the U2A beamline at the National Synchrotron Light Source (NSLS) of Brookhaven National Laboratory (BNL). The IR beam was focused onto the sample by a Bruker IR microscope, and then the spectrum was collected in transmission mode by the mercury cadmium telluride detector in the spectral range of $600-4000$ cm^{-1}. The resolution used in all IR measurements was 4 cm^{-1}. The thickness of the sample for IR measurement was 35 μm to allow sufficient IR transmission measurements. For all measurements, IR spectra were collected through a 30×30 μm^2 aperture. The reference spectrum, i.e., diamond anvil absorption at ambient pressure, was later divided as background from each sample spectrum to obtain the absorbance.

C. X-ray diffraction

XRD was used to identify reversible changes induced by increasing pressure as well as to validate our assumptions on the initial structure of the zinc and calcium phosphate used in the experiments. XRD spectra (at 30.55 keV; $\lambda = 0.4066$ nm) were collected under isotropic compression at the X17C beamline of the NSLS at BNL. To collect the spectra, a charge coupled device camera was used and the exposure time was set equal for all experiments to 400 s. The data were integrated using the FIT2D software and data analysis software such as POWDERCELL.

III. RESULTS

A. Identification of components of the thermal ZDDP decomposition product

The main objective of our study was to identify pressure induced structural transformations in the thermal decomposition product(s) of ZDDP and obtain the associated bulk modulus. As we show in this section, this task can be achieved more reliably if the complex spectroscopic features of the material can be related to model components and then analyzed independently. For this purpose we compared the x-ray and IR spectra of thermal decomposition products to the spectra of pyrophosphates and orthophosphates which have been previously identified to be reasonably representa-

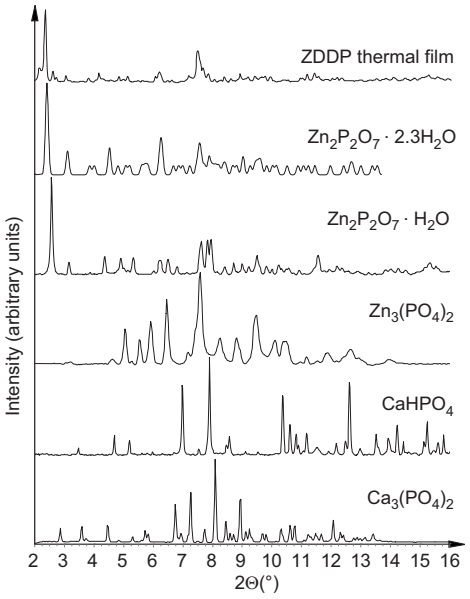

FIG. 1. Comparison of XRD spectra of various model compounds with the thermal decomposition product obtained from ZDDP in poly-α-olefin base oil solution. The XRD spectrum for $Zn_2P_2O_7 \cdot 2.3H_2O$ was reconstructed from the data reported in Ref. 33.

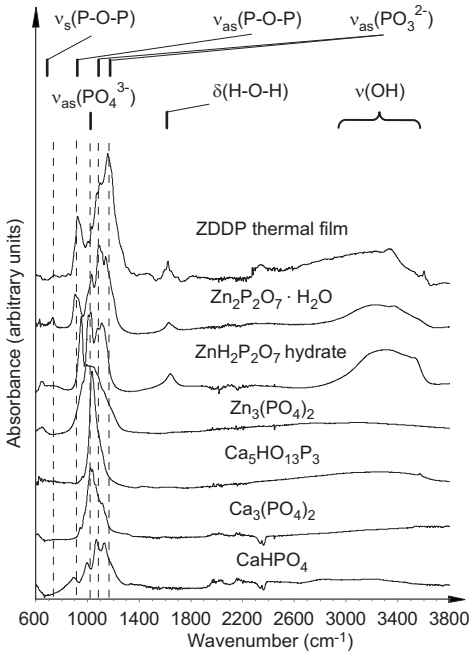

FIG. 2. Comparison of IR absorbance spectra of various model compounds with the thermal decomposition product obtained from ZDDP in poly-α-olefin base oil solution.

tive of the chemistry of the ZDDP decomposition products and tribofilms[5,32] (Fig. 1). Comparison with calcium phosphates allowed us to test whether any contamination of lubricating oil with calcium containing additives took place. Comparison of the spectroscopic features of the studied compounds with spectra of $Zn_2P_2O_7 \cdot 2.3H_2O$ (Ref. 33) and $Zn_2P_2O_7 \cdot H_2O$ indicates a very good agreement. We would like to emphasize that we used the experimental results reported in Ref. 33 to obtain the spectra of $Zn_2P_2O_7 \cdot 2.3H_2O$ shown in Fig. 1.

Following this description we can preliminarily conclude that ZDDP thermal decomposition product in the given conditions is a compound with diffraction features similar to the ones of the mixture of $Zn_2P_2O_7 \cdot 2.3H_2O$ and very small amount of $Zn_2P_2O_7 \cdot H_2O$. IR spectroscopy complements the XRD analysis with information about the short range structure of the thermal film. The IR analysis will help to identify vibrational modes of the PO_4 tetrahedra and OH groups and water molecules present in the film. It is important to remember that IR absorption in metal phosphates originates mostly from vibrations of the PO_4 tetrahedron. In metal phosphate hydrates we expect to see bands characteristic of water and OH vibrations.

In the metal phosphates under investigation, phosphorus always assumes tetrahedral coordination with four oxygen atoms building the PO_4 group. The PO_4 groups can be isolated or interconnected via one of the oxygen atoms (bridging oxygen atom). In a manner similar to the method used to classify silicates and aluminosilicates, the different phosphate tetrahedra can be classified according to their connectivities Q_n, where n is the number of bridging oxygen atoms per one PO_4 unit. In orthophosphates, pyrophosphates, and metaphosphates n equals, respectively, 0, 1, and 2.[34]

Using the previously published assignment of the bands[35,36] and our XRD data, we can further compare the material under current investigation with phosphate model compounds (see Fig. 2). IR spectroscopy supports the XRD data in terms of the similarity of the spectroscopic features of the thermal film and the crystalline zinc pyrophosphate hydrate. The latter contains solely $(P_2O_7)^{4-}$ anions (Q_1 species).[33,37] The characteristic vibrational mode of the $(P_2O_7)^{4-}$ are the Raman active symmetric stretching modes at 1016 and 1116 cm^{-1}. For detection of $(P_2O_7)^{4-}$ in IR spectroscopy, we can use the stretching bands of the bridging oxygen atoms: symmetric ν_s (P–O–P) at 739 cm^{-1} (see Fig. 2) and asymmetric ν_{as} (P–O–P) at 920 cm^{-1}. In addition to these two bands, the asymmetric stretching of end groups of the pyrophosphate $\nu_{as}(PO_3)^{2-}$ at 1056 cm^{-1} and at 1103–1155 cm^{-1} can be used. The primary use of the isobutyl ZDDP in our tests explains the absence of the characteristic band for metaphosphates[5] $(PO_2)^-$ groups (Q_2 species) which would be detected at 1200–1260 cm^{-1}.

The rest of our model compounds are orthophosphates and contain isolated $(PO_4)^{3-}$ ions (Q_0 species).[38–41] The latter can be characterized by a stretching band at 1029 cm^{-1} attributed to the A_g mode of the $(PO_4)^{3-}$ ion according to Frost.[42]

In phosphate hydrates the bands at 3542, 3473, 3338, and 3149 cm^{-1} can be assigned to hydroxyl stretching ν (OH) modes,[42,43] and the band at 1600 cm^{-1} is suggestive of the δ (H–O–H) bending mode. Additionally, the sharp band at 3600 cm^{-1} might indicate that a fraction of the OH groups do not participate in the hydrogen bonding, which indicates the possible presence of hydrogenated zinc (pyro)phosphates.

Despite the fact that IR spectra indicate the presence of some orthophosphate phase, we will continue our analysis using $Zn_2P_2O_7 \cdot 2.3H_2O$ phase, as the very strong signal of

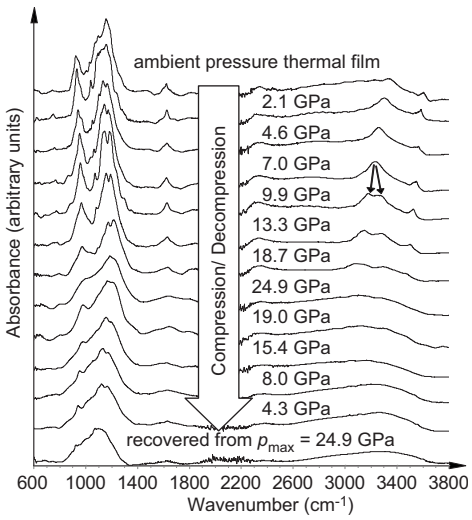

FIG. 3. IR absorbance spectra measured during a compression/decompression cycle of the thermal decomposition product obtained from ZDDP in poly-α-olefin base oil solution. The arrows highlight the splitting of spectroscopic features and are indicative of instability related to changes involving the hydroxyl groups.

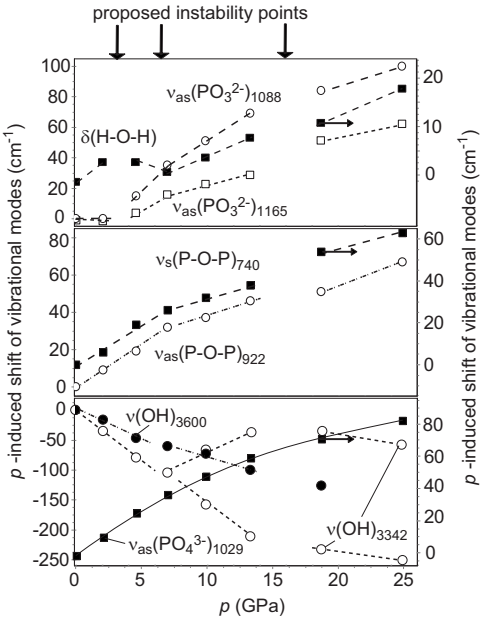

FIG. 4. Pressure induced shift in vibrational bands as a function of pressure. Evaluation of spectra shown in Fig. 3. Band assignments are explained in the text.

zinc pyrophosphate in both the IR analysis and XRD data indicates that the latter phase is dominant in the thermal film.

B. IR spectroscopy during compression

In this section we report the IR spectra of the thermal ZDDP decomposition product at various pressures during both compression and decompression (Fig. 3). These results will help to identify possible changes in vibrational modes and help to elucidate the details of the short range structure at each compression step.

Upon compression of the thermal film we see that the bands in the range of 740–1200 cm^{-1} representing vibrations of the phosphate groups exhibit a positive shift and a gradual smoothing of the features (Fig. 3). (By smoothing, we mean the loss of sharp structures in the spectra.) In contrast to the modes related to the phosphate groups, OH related modes exhibit a negative shift in the position of the stretching vibrations with increase in pressure. There is a transformation of the single peak feature at 3223 cm^{-1} into a double peak feature (3178 and 3280 cm^{-1}) at the compression step from 7 to 9.9 GPa. Dramatic smoothing of all spectroscopic features indicating possible amorphization of the compound occurs after a pressure increase to 24.9 GPa. The smoothing remains after decompression, indicating the irreversible character of the amorphization.

In order to gain more information about possible structural transformations we plotted the assigned IR bands of the thermal film as a function of pressure (Fig. 4). The asymmetric stretching bands $\nu_{as}(PO_3)^{2-}$ and bending vibrations δ (H–O–H) exhibit nonmonotonic pressure induced band shifts, indicating three pressure points at which possible transformations occur at 3 and 7 GPa and in the range between 14 and 18 GPa involving $(P_2O_7)^{4-}$ anions and hydroxyls. The first transition point indicates a change in the pressure-induced shift in δ (H–O–H) from positive to negative with increasing pressure as well as a positive shift in both $\nu_{as}(PO_3)^{2-}$ vibrations. The second point at about 7 GPa is characterized by the decrease in the pressure-induced rate change in the $\nu_{as}(PO_3)^{2-}$ mode and a change in the pressure dependence of the δ (H–O–H) vibration from negative to positive. Indication of a possible discontinuity in the pressure-induced shift in $\nu_{as}(PO_3)^{2-}$ at about 16 GPa is suggestive of a third transition point.

By contrast, the stretching bands of the OH groups ν(OH) and bridging oxygen vibrations ν_s (P–O–P) and ν_{as} (P–O–P) are suggestive of only two transformations at 7 and $\approx$16 GPa. It is conclusive that $(PO_4)^{3-}$ exhibit a smooth increase in frequency at a decreasing rate with increasing pressure, and there are no associated transitions. This is to be expected as isolated PO_4 groups have already been shown to be stable in the pressure range investigated here.[2,22] Verification of the transition pressures suggested by the IR transmission spectroscopy can be done with the help of the XRD analysis.

C. X-ray diffraction during compression

In this section we report the x-ray spectra of the thermal ZDDP decomposition product at various pressures during compression/decompression cycles (Fig. 5). The material is compressed and decompressed using three maximum pressures in order to obtain the pressure at which irreversible amorphization occurs. During the first compression, the maximum pressure is $\approx$12 GPa; during the next compression $p \approx 18$ GPa, and the maximum pressure is $\approx$24 GPa.

We analyze the spectra for pressure-induced crystal-crystal transformations or amorphization. The spectra shown in Fig. 5(a) indicate a slight pressure-induced reduction in the intensity and a shift in the spectral features to higher diffraction angles, indicating compression of the interplanar spacings. At 2.2 GPa, the peaks near $\approx$63° and $\approx$7.6° split, which will be discussed in the second last paragraph of this

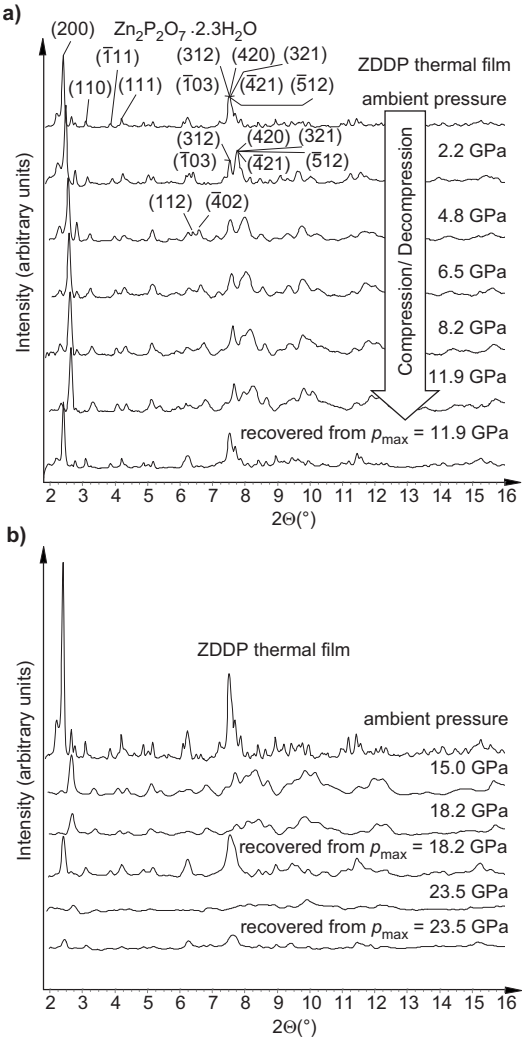

FIG. 5. XRD spectra of the studied material (thermal decomposition product obtained from ZDDP in poly-α-olefin base oil solution) during a compression/decompression cycle. (a) Maximum pressure in the experiment is ≈12 GPa. Only selected Bragg reflections are indexed. (b) Maximum pressures are ≈18 and ≈25 GPa, respectively.

section. Upon decompression from a maximum of ≈12 GPa back to ambient pressure, the spectra indicate full recovery of the original crystalline structure [Fig. 5(a)]. Otherwise no further dramatic changes in spectral shapes were detected until the pressure exceeded ≈18 GPa [Fig. 5(b)]. By contrast the spectra obtained after decompression from ≈18 GPa indicate a significant decrease in crystalline-specific intensities. In the following compression/decompression cycle to a maximum pressure of ≈24 GPa, the spectra indicate total and irreversible amorphization of the studied material.

In order to ascertain the equation of state (EOS) of the thermal film, which is shown in Fig. 6(a), we use the crystal data for $Zn_2P_2O_7 \cdot 2.3H_2O$ as a reference.[33] At ambient pressure, the same unit cell parameters are found as those stated in the literature;[33] to be specific, we use the monoclinic symmetry with unit cell parameters of $a=19.911$, $b=8.148$, $c=9.307$, and $\beta=102.89°$. To obtain the EOS, only four distinct reflections are used, i.e., (200), (110), $(\bar{1}11)$, and (111). As these peaks are mutually distant from one another, the risk of a misinterpretation due to the interference of the reflections at high Bragg angles is insignificant.

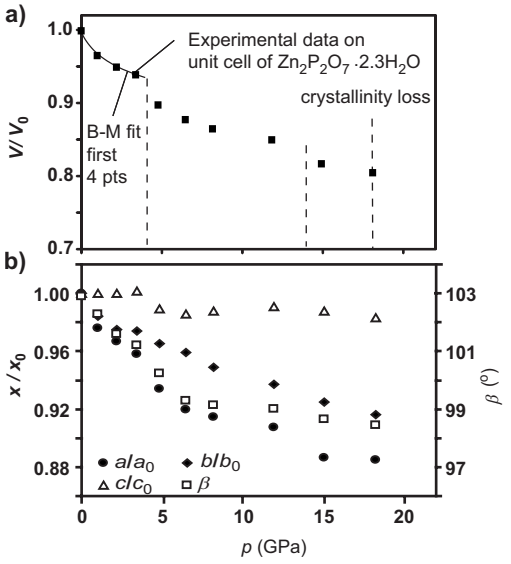

FIG. 6. (a) EOS as obtained from XRD experiments: fit of experimental data using the unit cell dimensions of $Zn_2P_2O_7 \cdot 2.3H_2O$ (Ref. 33). Bulk modulus $K(0)=24.8 \pm 3.1$ GPa at a rate of $K'(0)=27 \pm 10$. Dashed lines show the proposed transition points. (b) Relative unit cell parameters as a function of pressure. Included is the angle β of the monoclinic cell.

The EOS indicates two points of pressure-induced transitions at ≈5 and ≈15 GPa. The first four points of the EOS could be successfully used to calculate the bulk modulus and its pressure derivative, namely, $K(0)=24.8 \pm 3.1$ GPa at a rate of $K'(0)=27 \pm 10$. As shown in Fig. 6(b), the unit cell compression is not uniform. The material is the softest along the x-direction, i.e., the lattice parameter a changes the most with pressure, whereas it is stiffest along the z-direction. At the low-pressure transition just below 5 GPa, all unit cell parameters show a significant reduction. At the high-pressure transition near 15 GPa, the lattice parameter a shows the clearest discontinuity. Cell indexing analysis reveals that the nonuniform deformation of the unit cell [see Fig. 6(b)] concluded from the (200), (110), $(\bar{1}11)$, and (111) peaks is consistent with the splittings of the (420), $(\bar{4}21)$, (321), and $(\bar{5}12)$ reflections near 2.2 GPa, which are shown in Fig. 5(a). A similar comment applies to the splitting of the (112) and $(\bar{4}02)$ reflections.

Comparison of the data obtained with IR spectroscopy and XRD indicates that there are probably two transition points. Observation of full recovery of the XRD pattern after decompression from $p_{max}=12$ GPa coupled with the IR observations leads to the conclusion that the compound undergoes a displacive crystal-crystal transition at about 5 GPa due to instabilities associated with the OH groups. Because of the fact that the OH groups only insignificantly contribute to x-ray scattering, the spectral features measured with XRD do not indicate significant changes, rather a discontinuity in the EOS. The discontinuous behavior of the vibrational frequencies of the OH and pyrophosphate with pressure (as analyzed by IR spectroscopy, see Fig. 4) makes us conclude that the second transition near 15 GPa is driven by additional instabilities of these groups.

IV. CONCLUSIONS

In our experiments, we observed that the thermal decomposition product of the ZDDP in base oil solution is mainly consistent with $Zn_2P_2O_7 \cdot 2.3H_2O$ together with possible minor amounts of hydrogenated Zn phosphates and orthophosphates. By evaluation of the EOS with the help of the Birch–Murnaghan[44] relation, we obtained a bulk modulus at ambient pressure of $K(0)=24.8\pm3.1$ GPa. The resulting bulk modulus very closely reflects the values ($K=25$ GPa) obtained from nanoindentation experiments on tribofilms located in the valleys between the tops of the antiwear pads.[14] Although the $Zn_2P_2O_7 \cdot 2.3H_2O$ is relatively compliant under ambient conditions, it stiffens rapidly under increasing pressure p, exhibiting stiffening at $K'(0)=27\pm10$. In addition, its original crystalline structure becomes thermodynamically unstable at a relatively small pressure $p\approx5$ GPa, at which point it undergoes a reversible displacive crystal-crystal transition due to instability associated with the hydroxyl groups. At a pressure in the vicinity of 15 GPa, the system undergoes an additional transition possibly connected with instability of both hydroxyl groups and bending modes of the $(P_2O_7)^{4-}$ anions. Upon further compression above 19 GPa, the system amorphizes irreversibly.

In order to understand the molecular mechanism of stiffening and observed transitions, we wish to remind the reader that the main building blocks in metal phosphates are phosphate units (in $Zn_2P_2O_7 \cdot 2.3H_2O$ there are pyrophosphate groups—two PO_4 tetrahedra sharing one bridging oxygen), which are interconnected at the cation site. The stability of the isolated PO_4 groups in the pressure range investigated here has been previously verified by high pressure experiments and *ab initio* calculations[2,22] (also see IR spectra reported here). Similarly, IR spectroscopy indicates pressure-induced changes only on the bending modes of the pyrophosphate groups, leaving the PO_4 groups unchanged. Previously,[2,12] we have argued that there are two sites that can improve the interconnection of the phosphates (degree of polymerization or cross linking), thereby increasing the bulk modulus—the cation site (the cation coordination) and the bridging oxygen site. Increase in the concentration of bridging oxygen sites increases the chain length of the phosphates; however, in order to achieve the effect of stiffening, the interconnected phosphates should form a three dimensional network. Hydrogenation or hydration of the phosphates counters the interconnection of the phosphate units, i.e., the degree of polymerization or cross linking will be reduced, resulting in a decrease in the bulk modulus.

The above arguments can be used to understand differences in the bulk modulus of the metal phosphates at ambient conditions reported earlier[12] and those described here as dependent on the degree of "cross linking." Applying this argument, we can see that hydration reduces the degree of cross linking of the phosphates, thereby reducing the bulk modulus from ≈90 GPa (Ref. 12) ($Zn_2P_2O_7 \cdot H_2O$) to ≈25 GPa ($Zn_2P_2O_7 \cdot 2.3H_2O$).

To further understand the mechanism of stiffening upon compression it is worth recollecting two facts: (a) the bulk modulus is dominated by repulsive interactions, in particular, at high pressures (as one can easily ascertain from calculating the bulk modulus of a Lennard-Jones system) and (b) the softest components in a system (or the weakest repulsion between correlated units) mainly determines the compliance of the system. Quick compression of the compliant sites results in rapid increase in the structural confinement of the phosphates which then results in a rapid increase in bulk modulus. Our previously published idea[12] that a phosphate network is destabilized when the free volume corresponding to the ligands and cations is consumed by the compression, the network starts to respond with elastic properties of the phosphate units [210 ± 40 GPa (Ref. 12)], is also supported by experiments presented here. Namely, the presence of hydroxyl groups makes the whole system become relatively soft. Once pressure reaches a critical value (the network responds with the elastic properties of phosphates) hydroxyls are the sites where the system becomes destabilized in the first place.

In our previous study, the $Zn_2P_2O_7 \cdot H_2O$ data did not indicate any crystal-crystal transitions,[12] and thus we would argue that in order for such transitions to take place, the unit cell should contain a critical number of compliant sites (in our case hydroxyls), a condition unmet in the monohydrate.

Whether the system undergoes a reversible crystal-crystal transition or amorphizes depends on what site is responsible for the thermodynamic instability of the unit cell. Our previous experimental data, as well as the data shown here, lead us to conclude that instabilities affecting the cation site and bridging oxygen would lead to irreversible pressure-induced transitions such as amorphization. According to experiment, the pressure at which amorphization occurs increases with increasing initial cation coordination. By contrast, the instability on the H or OH sites would lead to displacive crystal-crystal transition, as they do not participate in network formation and these can occur before the pressure required for amorphization is reached.

We believe that the antiwear function of the ZDDP based film is connected with its ability to stiffen rapidly under pressure[12,13] because stiffening reduces the effect of inertial confinement, i.e., the substrate can start to deform while interacting with a relatively soft film, which reduces the maximum pressure achieved during the collision of two asperities. One could argue that one single material, which stiffens under pressure, behaves elastically like a system of various layers with different stiffness, thereby producing what we might term a "helmet effect." We further believe that the dynamical response of the material on the time scale of asperity collision is important in antiwear action and should be studied.

The origin of the observed smart material behavior can be related to the decrease in the flexibility of rigid unit modes upon compression—with or without change in cation coordination. The smart behavior of the antiwear film appears to be induced due to a low initial bulk modulus in the presence of OH groups and an open network structure. As we found previously, the stiffening under pressure is particularly strong for four-coordinated and hydrogenated metal phosphates but can also be strong for hydrates if the concentration of OH groups exceeds a critical value.

With regard to the influence of phosphate hydration, we would like to indicate that our results might deliver new understanding of the increased stiffness of the tribofilms on top of the pads observed earlier.[14,15] However, given that our conclusion is based on only one parameter (bulk modulus), we wish to emphasize the speculative nature of this statement. It seems as if shear-induced amorphization of the tops of the pads (the film is believed to form preferentially on top of the original asperities present at the sliding interfaces) might induce dehydration of the initially crystalline structure and increase the degree of polymerization or cross linking of the phosphates with subsequent increase in the film stiffness. Even if shear effects are not directly responsible, energy dissipation would lead to the highest temperatures at the contact points which could also lead to dehydration. Either or both processes could transform $Zn_2P_2O_7 \cdot 2.3H_2O$ into $Zn_2P_2O_7 \cdot H_2O$ or $Zn_2P_2O_7$, subsequently increasing the bulk modulus at ambient conditions.

ACKNOWLEDGMENTS

M.H.M. and Y.S. wish to acknowledge the support from the Natural Sciences and Engineering Research Council of Canada and M.H.M. from Premiers Research Excellence Award. The research described in this manuscript was performed partially at the National Synchrotron Light Source of Brookhaven National Laboratory. In this regard we are grateful to the National Synchrotron Light Source and especially to Z. Lu and J. Hu for their technical support and expertise. We also thank Yue-Rong Li for help in preparation of the ZDDP decomposition products.

[1] H. Spikes, Tribol. Lett. **17**, 469 (2004).
[2] N. J. Mosey, M. H. Müser, and T. K. Woo, Science **307**, 1612 (2005).
[3] P. A. Willermet, D. P. Dailey, R. O. Carter, P. J. Schmitz, and W. Zhu, Tribol. Int. **28**, 177 (1995).
[4] M. A. Nicholls, T. Do, P. R. Norton, M. Kasrai, and G. M. Bancroft, Tribol. Int. **38**, 15 (2005).
[5] M. Fuller, Z. F. Yin, M. Kasrai, G. M. Bancroft, E. S. Yamaguchi, P. R. Ryason, P. A. Willermet, and K. H. Tan, Tribol. Int. **30**, 305 (1997).
[6] Z. F. Yin, M. Kasrai, M. Fuller, G. M. Bancroft, K. Fyfe, and K. H. Tan, Wear **202**, 172 (1997).
[7] J. M. Martin, Tribol. Lett. **6**, 1 (1999).
[8] H. Fujita and H. A. Spikes, Tribol. Trans. **48**, 567 (2005).
[9] M. Z. Huq, X. Chen, P. B. Aswath, and R. L. Elsenbaumer, Tribol. Lett. **19**, 127 (2005).
[10] K. Varlot, M. Kasrai, J. M. Martin, B. Vacher, G. M. Bancroft, E. S. Yamaguchi, and P. R. Ryason, Tribol. Lett. **8**, 9 (2000).
[11] B. Dacre and C. H. Bovington, ASLE Trans. **25**, 546 (1982).
[12] D. Shakhvorostov, M. H. Müser, and N. J. Mosey, Phys. Rev. B **79**, 094107 (2009).
[13] S. Bec, A. Tonck, J. M. Georges, R. C. Coy, J. C. Bell, and G. W. Roper, Proc. R. Soc. London, Ser. A **455**, 4181 (1999).
[14] O. L. Warren, J. F. Graham, P. R. Norton, J. E. Houston, and T. A. Michalske, Tribol. Lett. **4**, 189 (1998).
[15] M. A. Nicholls, G. M. Bancroft, P. R. Norton, M. Kasrai, G. D. Stasio, B. H. Frazer, and L. M. Wiesec, Tribol. Lett. **17**, 245 (2004).
[16] Z. F. Yin, M. Kasrai, G. M. Bancroft, K. F. Laycock, and K. H. Tan, Tribol. Int. **26**, 383 (1993).
[17] Z. F. Yin, M. Kasrai, G. M. Bancroft, K. H. Tan, and X. H. Feng, Phys. Rev. B **51**, 742 (1995).
[18] M. Aktary, M. T. McDermott, and J. Torkelson, Wear **247**, 172 (2001).
[19] Y.-R. Li, G. Pereira, A. Lachenwitzer, M. Kasrai, and P. R. Norton, Tribol. Lett. **29**, 11 (2008).
[20] N. J. Mosey, T. K. Woo, and M. H. Müser, Phys. Rev. B **72**, 054124 (2005).
[21] N. J. Mosey, T. K. Woo, M. Kasrai, P. R. Norton, G. M. Bancroft, and M. H. Müser, Tribol. Lett. **24**, 105 (2006).
[22] D. Shakhvorostov, M. H. Müser, N. J. Mosey, D. J. Munoz-Paniagua, G. Pereira, Y. Song, M. Kasrai, and P. R. Norton, J. Chem. Phys. **128**, 074706 (2008).
[23] K. Takemura and A. Dewaele, Phys. Rev. B **78**, 104119 (2008).
[24] G. Misra, P. Tripathi, and S. C. Goyal, Philos. Mag. Lett. **87**, 393 (2007).
[25] L. G. Liu, Mech. Mater. **14**, 283 (1993).
[26] S. N. Vaboya and G. C. Kennedy, J. Phys. Chem. Solids **31**, 2329 (1970).
[27] S. Raju, E. Mohandas, and V. S. Raghunathan, J. Phys. Chem. Solids **58**, 1367 (1997).
[28] M. T. Dove, A. P. Giddy, and V. Heine, Ferroelectrics **136**, 33 (1992).
[29] K. D. Hammonds, M. T. Dove, A. P. Giddy, V. Heine, and B. Winkler, Am. Mineral. **81**, 1057 (1996).
[30] H. K. Mao, P. M. Bell, J. W. Shaner, and D. J. Steinberg, J. Appl. Phys. **46**, 543 (1978).
[31] B. M. Nirsha, T. V. Khomutova, A. A. Fakeev, B. V. Zhadanov, V. M. Agre, N. P. Kozlova, and V. A. Olikova, Russ. J. Inorg. Chem. **27**, 630 (1982).
[32] P. A. Willermet, R. O. Carter, and E. N. Boulos, Tribol. Int. **25**, 371 (1992).
[33] B. M. Nirsha, T. V. Khomutova, A. A. Fakeev, V. M. Agre, B. V. Zhadanov, G. R. Allakhverdov, N. P. Kozlova, and V. A. Olikova, Russ. J. Inorg. Chem. **25**, 213 (1980).
[34] A. Durif, *Crystal Chemistry of Condensed Phosphates*, 1st ed. (Plenum, New York, 1995).
[35] R. K. Brow, D. R. Tallant, S. T. Myers, and C. C. Phifer, J. Non-Cryst. Solids **191**, 45 (1995).
[36] G. Le Saoût, P. Simon, F. Fayon, A. Blin, and Y. Vaills, J. Raman Spectrosc. **33**, 740 (2002).
[37] B. E. Robertson and C. Calvo, J. Solid State Chem. **1**, 120 (1970).
[38] C. Calvo, Can. J. Chem. **43**, 436 (1965).
[39] G. MacLennan and C. A. Beevers, Acta Crystallogr. **8**, 579 (1955).
[40] W. A. Denne and D. W. Jones, J. Chem. Cryst. **1**, 347 (1971).
[41] M. Yashima, A. Sakai, T. Kamiyama, and A. Hoshikawa, J. Solid State Chem. **175**, 272 (2003).
[42] R. L. Frost, Spectrochim. Acta, Part A **60**, 1439 (2004).
[43] O. Pawlig, V. Schellenschlager, H. D. Lutz, and R. Trettin, Spectrochim. Acta, Part A **57**, 581 (2001).
[44] F. Birch, Phys. Rev. **71**, 809 (1947).